Research

Author for correspondence:
Marcin Karbarz
e-mail: karbarz@chem.uw.edu.pl

Synthesis of cross-linked poly(acrylic acid) nanogels in an aqueous environment using precipitation polymerization: unusually high volume change

Marcin Mackiewicz, Zbigniew Stojek and Marcin Karbarz

Faculty of Chemistry, Biological and Chemical Research Center, University of Warsaw, 101 Żwirki i Wigury Avenue, 02-089 Warsaw, Poland

MK, 0000-0002-7813-0513

For the first time, by using precipitation polymerization in an aqueous solution, a cross-linked poly(acrylic acid)—(pAA) nanogel was synthesized. pAA was synthesized and cross-linked with N,N'-methylenebisacrylamide (BIS) at 70°C in an acidified environment (pH 2) and containing 0.7 M NaCl using potassium persulfate as the initiator. Ionized pAA was soluble in water. The use of sodium chloride at low pH caused a decrease in the solubility of pAA and led to its precipitation and formation of cross-linked pAA nanogel. By using electron microscopies and light scattering techniques, the morphology, pH sensitivity and zeta potential of the obtained p(AA-BIS) nanogel were evaluated. The polymerization in an aqueous environment resulted in a very big swelling/shrinking coefficient (of approx. 4000) in response to pH and exhibited an unusually high negative zeta potential (of approx. −130 mV). These properties make the nanogel a very interesting sorbent and a construction material.

1. Introduction

Micro- and nanogels are cross-linked polymers of micro–nanosize filled with a solvent. They can exist either in the swollen or the shrunken state depending on the environmental conditions [1–4]. They exhibit very high surface areas, low viscosities and, compared with regular gels, can be injected into the body. They are characterized by a rapid and large-magnitude volume phase transition in response to changes in environmental conditions

such as temperature, ionic strength, pH and the redox state of the polymer [5–9]. Gels' sensitivity to environmental parameters is dependent on their functional components. Micro- and nanogels have great potential in applications in areas such as drug carriers, [10–13] catalysis [14,15] and sensors [16,17]. Micro- and nanogels containing carboxylic groups are capable of further modification and loading of active substances.

Cross-linked poly(acrylic acid)—p(AA) particles are examples of nanogels sensitive to pH. Due to the presence of a high amount of carboxylic groups, pAA gels undergo a big-volume transition in response to appropriate pH changes [18]. At pH smaller than pK_a of pAA (4.5) [19], they exist in the shrunken state (carboxylic groups are protonated), while at pH higher than pK_a they are swollen (carboxylic groups are dissociated).

The soft, swollen network of pAA nanogels, their hydrophilic nature and viscous consistency are similar to biological tissues. Additionally, their surface tension in biological fluids is low, they are biocompatible and have a reticulated structure. Because of these properties pAA gels are used in medicine as anticorrosion films for covering implants, as skin disease- or care materials, as high-bonding-strength medical glue [20–22] and especially as drug carriers [23]. The ability of pAA to adhere, for a long time, to biological tissues (bio(muco)adhesion) increases the drug absorption in the target site [24]. pAA gels are used in bioadhesive pharmaceutical hydrogels and sold as Polycarbophil or Carbopol [25,26]. The important property of pAA gels is that their polyanionic charge allows for easy and highly efficient loading of cationic substances [27] and allows them to combine with proteins and enzymes.

pAA nanogels are synthesized mainly by using microemulsion polymerization and distillation polymerization in a two-phase organic liquid/water medium with the help of stabilizers [28,29]. Ahmed *et al.* synthesized pAA nanogels via inverse-phase microemulsion polymerization at 70°C in liquid paraffin [30]. Tween 80 and Span 80 served as nonionic surfactants and azobisisobutyronitrile (AIBN) served as the initiator. The aqueous phase contained AA and *N,N′*-methylenebis(acrylamide) (BIS) as the cross-linking agent. These nanogels were used to adsorb cellulase, to enhance cellulase's efficacy and stability. In other work, Seyedeh *et al.* synthesized pAA nanogel to be used as a drug carrier. They used the distillation precipitation polymerization process with BIS as the linker [31]. Acetonitrile and AIBN were used as the solvent and the initiator, respectively. The reaction was performed at the boiling point of acetonitrile. We want to emphasize that, up to now, there is no report on the successful synthesis of pAA nanogel in just water.

As an environmentally-protective measure, the synthesis should be carried out in water and this was only partially possible. Acrylic acid was added as the comonomer during the emulsion polymerization of *N*-isopropylacrylamide (NIPA) and *N,N*-diethylacrylamide (DEA) [32–37]. Unfortunately, the molar content of AA in these gels did not exceed 40%. Moreover, the majority of micro- and nanogels containing ionized comonomers did not exhibit a high swelling degree. Even in the case of pure pAA, despite the fact that they consisted mainly of ionized groups, the swelling degree was not so high and their zeta potential did not exceed −60 mV [38,39].

The aim of this paper was to synthesize pure pAA nanogels in aqueous solution without the use of any toxic surfactants and stabilizers. We managed to synthesize pAA nanogel cross-linked with BIS using the precipitation polymerization process carried out in an aqueous environment without the addition of surfactants. We used sodium chloride and maintained low pH during the polymerization process to decrease the solubility of pAA and to precipitate it to form the nanogel. The nanogel exhibited very high volume change in response to pH and a very negative charge (zeta potential was approx. −130 mV at pH higher than pK_a). The reported values in the literature are much less negative [40–47].

2. Experimental

2.1. Chemicals

Acrylic acid (AA, 99%), potassium persulfate (KPS, 99.99%) and *N,N′*-methylenebis(acrylamide) (BIS, 99%) were supplied by Aldrich. NaOH (99%), HCl (35–38%) and NaCl (99%) were purchased from POCh. All ingredients were used as received. High-purity water was used for the preparation of all solutions. Water was purified with a Hydrolab/HLP purification system; the final conductivity of the water was 0.055 µS cm^{-1}.

2.2. Nanogel synthesis

The precipitation polymerization process, used in the synthesis of other smart polymers [48], was selected by us to obtain poly(AA-BIS) nanogels in aqueous media (scheme 1). AA and BIS were dissolved in 50 ml
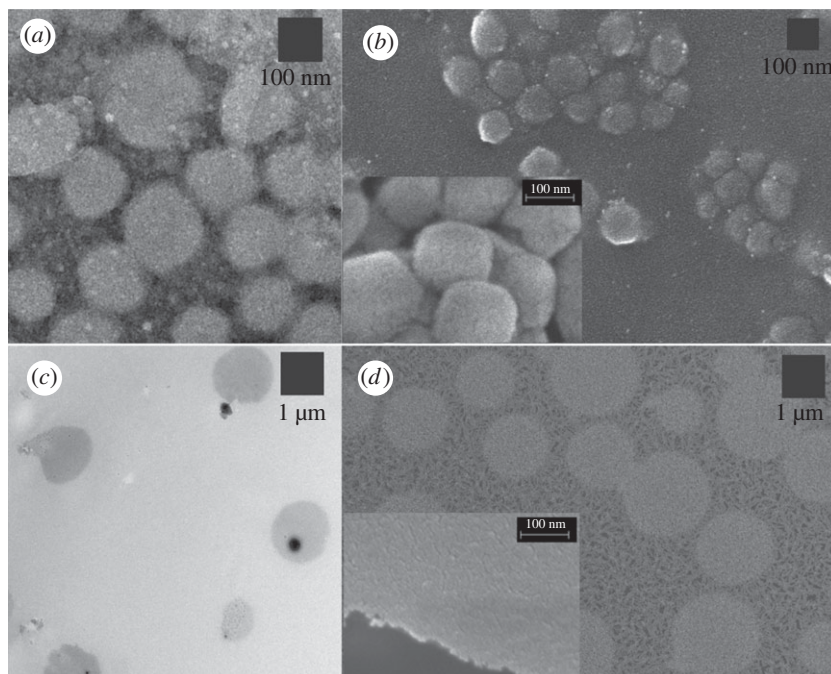
Scheme 1. Synthesis of poly(AA-BIS) nanogels.

of deionized water and placed in a flask equipped with a reflux condenser, an inlet- and an outlet of argon and a magnetic stirrer. Next, NaCl was added and the pH was set to a value of 2 by adding an appropriate amount of HCl to decrease the solubility of pAA. The final concentration of sodium chloride was 0.7 M. Other pH and ionic strength did not lead to better results. The mixture of reactants was heated at 70°C and deoxygenated for 30 min. Next, 13.5 mg of KPS was added to initiate polymerization. The molar linker/AA ratio and the total concentration of the monomers were optimized to get acceptable polydispersity with the monomodal size distribution of the particles. We found that the molar linker/AA ratio of 0.01 and the total concentration of the monomers of 420 mM were optimal.

The reaction was carried out for 24 h under a blanket of argon. The stirring rate was set at 250 r.p.m. The unstable, bigger particles formed a sediment (it took 1 day) and in this way were removed. The stable fraction of the nanogel was purified by using glass wool and finally by dialysis. In the dialysis process, dialysis bags of 10 kDa molecular weight cut-off (Spectra/Por®) were used. The gel samples were dialysed with 5 l of water for three weeks at room temperature; water was changed daily. The yield of pAA nanogels, as compared to the initial AA monomer quantity, was approximately 50%. It was obtained gravimetrically after the separation of the purified nanogels.

2.3. Instrumental

2.3.1. Dynamic light scattering

A Malvern Zetasizer instrument (Nano ZS, UK) equipped with a 4-mW Helium-Neon laser with a wavelength of 632.8 nm and a scattering angle of 173° was used to determine the hydrodynamic diameter of the nanogel particles. The samples were kept at selected temperatures for 5 min before the measurements.

The pH of aqueous suspensions of nanogels was adjusted by adding either NaOH or HCl and was monitored just before the measurements using a Mettler Toledo, model SevenGo-SG2 pH-meter. Ionic strength was kept constant (0.09 M).

2.3.2. Electron microscopy (SEM and TEM)

A Merlin (Zeiss) instrument working at 3 kV was used to take SEM micrographs. A drop of the nanogel emulsion of pH *ca* 3 was placed on the SEM-sample holder and left to dry at RT. Before the measurements, the samples were coated with a 5-nm layer of the Au–Pd alloy deposited in vacuum using a Mini Sputter Coater (Polaron SC7620).

TEM micrograms were taken with a Libra 1200 (Zeiss) instrument. The accelerating voltage was 120 kV. A drop of nanogel dispersion of pH *ca* 3 was placed on a formvar-coated copper grid. Then samples were left to dry at RT. Brightfield (the contrast mode) was used for taking both SEM and TEM micrographs.

3. Results and discussion

The morphology of dried p(AA-BIS) nanogels was examined with electron microscopies. TEM and SEM micrographs of the dried nanogel emulsion of pH *ca* 3 are presented in figure 1*a,b*, respectively. At pH 3,

Figure 1. TEM (*a,c*) and SEM (*b,d*) micrographs of dried p(AA-BIS) nanogels at pH 3 (*a,b*) and pH 11 (*c,d*). Insets in (*b,d*): higher magnification allowing presentation and comparison of porosity of particle surfaces. SEM pictures were taken using mixed detectors: In-Lens and HE-SE2.

almost all carboxylic groups are protonated and nanogels are shrunken. As can be seen in the micrographs, the nanogel particles were more or less spherical. The mean sizes of the particles obtained from the SEM and TEM micrographs at pH 3 equalled 99 ± 11 (30 particles) and 137 ± 22 nm (13 particles), respectively. The micrographs of dried nanogel emulsion of pH *ca* 11 are presented in figure 1*c,d*. At pH 11 the nanogels were swollen (carboxylic groups were dissociated). The nanogel particles were spherical and their size was greater than 1 µm. The mean sizes of the particles obtained from the SEM and TEM micrographs equalled 1523 ± 260 nm (15 particles) and 1293 ± 293 nm (5 particles), respectively.

Next, the sensitivity of the nanogel to pH was examined using the DLS technique. The plot of the hydrodynamic diameter of the p(NIPA-BIS) nanogel as a function of pH is presented in figure 2*a*. Since pK_a of carboxylic groups in pAA chains is approximately 4.5 [19], therefore at pH lower than pK_a, the diameter of the nanogel particles should be smaller than the diameter at pH above pK_a. As can be seen from figure 2*a*, the diameter of the nanogel did not change significantly below pH 4 and above pH 7. The biggest changes in the size of the nanogel were observed at pH in the range of 4–7. Apparently, the nanogel exhibited very high swelling changes. For example, the hydrodynamic diameter of the nanogel measured at pH 2 and pH 8 equalled 122 nm and 1990 nm, respectively. So, the change in the volume of the nanogel was more than three orders of magnitude; the nanogels swelled more than 4000 times. This was calculated by dividing the third powers of hydrodynamic diameters of the particles at pH 8 and 2 $(1990 \text{ nm})^3/(122 \text{ nm})^3$. Moreover, the nanogels were stable for a long time; therefore, for example, the sizes of particles measured at pH 2 and pH 8 after approximately one month were 131 ± 60 nm and 1897 ± 190 nm, respectively. Importantly, the hydrodynamic diameter is the size of particles with the hydration shells. Thus, this size of particles is rather bigger than the size of dried particles measured by using SEM and TEM. Higher magnification of the particles is presented in the insets in figure 1*b,d* to allow comparison of the porosity of the nanoparticles in pH 2 and 8.

Nanogel in the shrunken state, at acidic pH, formed a turbid aqueous emulsion, while its solution in the swollen state, at alkaline pH, was transparent. pH increase from 2 to 8 caused the polydispersity index to increase from 0.10 to 0.25. Typical size distributions of the nanogels measured at two selected pHs are presented in figure 2*b*.

The high swelling degree of the nanogel was related to the high amount of carboxylic groups in the polymer network and the corresponding, after dissociation, high negative charge. We investigated the
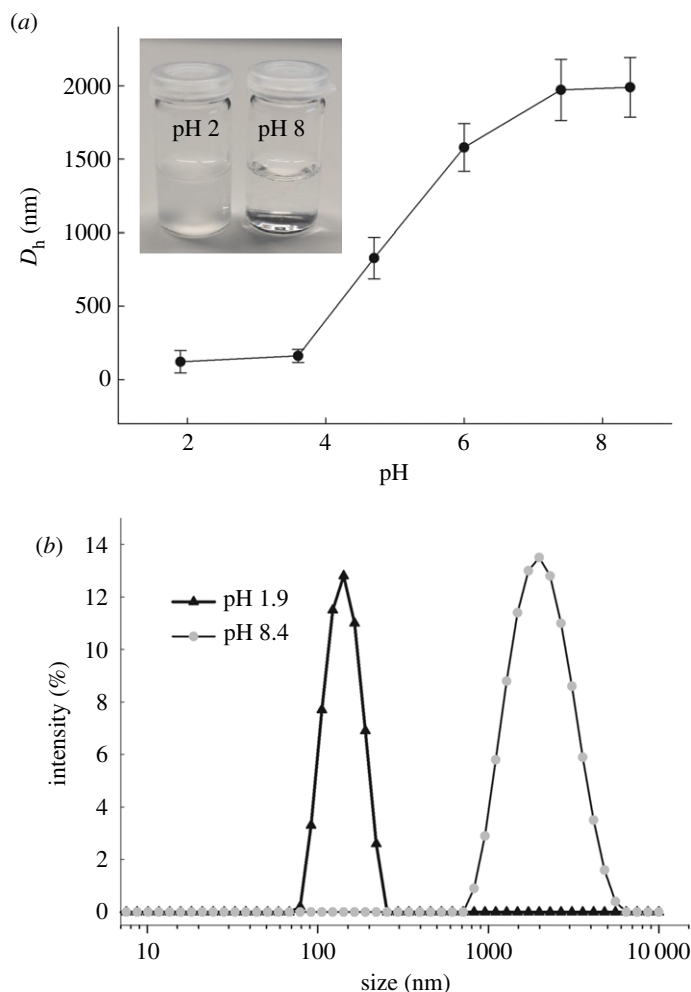
Figure 2. (a) Hydrodynamic diameter (D_h) of p(AA-BIS) nanogel (at 25°C) plotted versus pH. (b) Micro-/nanogel size distributions measured at two selected values of pH. Inset—optical images of nanogel emulsions in the shrunken and swollen states taken at two selected pHs. Ionic strength was kept constant at 90 mM.

zeta potential of the nanogel at different pHs. The obtained data are shown in figure 3. As can be seen, the nanogel exhibited an unusually big change in the zeta potential as the pH was increased. In an acidic environment, most of the carboxylic groups were protonated and the zeta potential was close to 0. A drastic decrease in the zeta potential (approx. −130 mV) was observed in the range of pH from approximately 4–8, where the carboxylic groups were deprotonated. The zeta potential dropped so much with that increase in pH because of the ionization of carboxylic groups and thus the corresponding increase in the negative charge.

4. Conclusion

We have demonstrated that with the application of proper conditions, there is a possibility for the synthesis of the cross-linked pAA nanogel in the aqueous environment. The obtained pH-sensitive p(AA-BIS) nanogel consisted of poly(acrylic acid) cross-linked with *N*,*N*′-methylenebisacrylamide. The precipitation polymerization process was used. It was carried out at 70°C and at pH 2 in water containing sodium chloride. pH 2 and the presence of sodium chloride caused a substantial decrease in the solubility of pAA, and thus enabled us to obtain the insoluble, cross-linked pAA nanogel. Thanks to conducting the polymerization in the aqueous solution, the obtained spherical particles of the nanogel exhibited unusually high sensitivity to pH. In the swollen state, the particle diameter was approximately 14 times bigger (changed from 122 nm at pH 2 to 1990 nm at pH 8) than in the shrunken state. So, the nanogel swelled more than 4000 times when the environment was changed from acidic to basic. This number can be compared with the swelling/shrinking ratio of the nanogels obtained in the traditional organic medium,
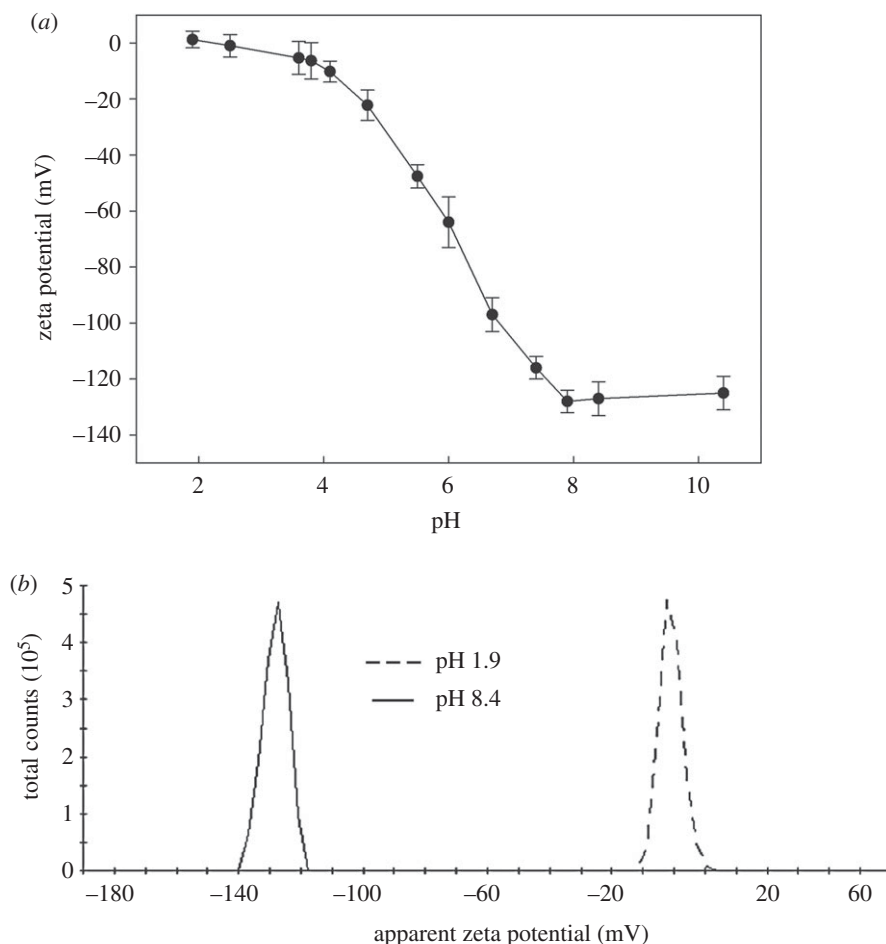
Figure 3. (*a*) Zeta potential of p(AA-BIS) nanogel measured versus pH at 25℃. Ionic strength was kept constant at 90 mM. Standard deviations indicated in the plot were estimated from three independent measurements. (*b*) Distribution of zeta potential measured for nanogel at two selected pH values.

where it was limited to the range of 7–25 [30,31,49,50]. The reason for this difference could be the presence of organic impurities in the gels. We want to add that the nanogel obtained in the aqueous environment also exhibited an unusually negative zeta potential at basic pH; it reached approximately −130 mV. In the future, we want to use this nanogel as a high-loading-capacity drug nanocarrier sensitive to pH.

References

1. Chen GH, Hoffman AS. 1995 Graft-copolymers that exhibit temperature-induced phase-transitions over a wide-range of pH. *Nature* **373**, 49–52. (doi:10.1038/373049a0)

2. Mackiewicz M, Marcisz K, Strawski M, Romanski J, Stojek Z, Karbarz M. 2018 Modification of gold electrode with a monolayer of self-assembled microgels. *Electrochim. Acta* **268**, 531–538. (doi:10.1016/j.electacta.2018.02.127)

3. Snowden MJ, Chowdhry BZ, Vincent B, Morris GE. 1996 Colloidal copolymer microgels of N-isopropylacrylamide and acrylic acid: pH, ionic strength and temperature effects. *J. Chem. Soc. Faraday Trans.* **92**, 5013–5016. (doi:10.1039/Ft9969205013)

4. Saunders BR, Vincent B. 1999 Microgel particles as model colloids: theory, properties and applications. *Adv. Colloid Interface Sci.* **80**, 1–25. (doi:10.1016/S0001-8686(98)00071-2)

5. Mackiewicz M, Romanski J, Karbarz M. 2014 New ampholytic microgels based on N-isopropylacrylamide and alpha-amino acid: changes in swelling behavior as a function of temperature, pH and divalent cation concentration. *Rsc Adv.* **4**, 48 905–48 911. (doi:10.1039/c4ra08924c)

6. Tian YF, Bian SS, Yang WL. 2016 A redox-labile poly(oligo(ethylene glycol)methacrylate)-based nanogel with tunable thermosensitivity for drug delivery. *Polym. Chem.* **7**, 1913–1921. (doi:10.1039/c6py00057f)

7. Mackiewicz M, Romanski J, Drozd E, Gruber-Bzura B, Fiedor P, Stojek Z, Karbarz M. 2017 Nanohydrogel with N,N′-bis(acryloyl)cystine crosslinker loading for high drug. *Int. J. Pharm.* **523**, 336–342. (doi:10.1016/j.ijpharm.2017.03.r031)

8. Zhang H, Zhai YJ, Wang J, Zhai GX. 2016 New progress and prospects: the application of nanogel in drug delivery. *Mater. Sci. Eng. C Mater. Biol. Appl.* **60**, 560–568. (doi:10.1016/j.msec.2015.11.041)

9. Mackiewicz M, Stojek Z, Karbarz M. 2017 Unusual swelling behavior of core-shell microgels built from polymers exhibiting lower critical solubility temperature. *Eur. Polym. J.* **95**, 314–322. (doi:10.1016/j.eurpolymj.2017.08.011)

10. Zhang LP, Xi L, Shi G, Zhu CP, Ni CH. 2016 Reduction-responsive zwitterionic nanogels based on carboxymethyl chitosan for enhancing cellular uptake in drug release. *Colloid. Polym. Sci.* **294**, 629–637. (doi:10.1007/s00396-015-3822-2)

11. Mackiewicz M, Kaniewska K, Romanski J, Augustin E, Stojek Z, Karbarz M. 2015 Stable and degradable microgels linked with cystine for storing and environmentally triggered release of drugs. *J. Mater. Chem. B* **3**, 7262–7270. (https://doi.org/10.1039/C5TB00907C)

12. Jin S, Wan JX, Meng LZ, Huang XX, Guo J, Liu L, Wang CC. 2015 Biodegradation and toxicity of protease/redox/pH stimuli-responsive PEGlated PMAA nanohydrogels for targeting drug delivery. *ACS Appl. Mater. Interfaces* **7**, 19 843–19 852. (doi:10.1021/acsami.5b05984)

13. Perez E, Olmo R, Teijon C, Muniz E, Montero N, Teijon JM, Blanco MD. 2015 Biocompatibility evaluation of pH and glutathione-responsive nanohydrogels after intravenous administration. *Colloid Surf. B* **136**, 222–231. (doi:10.1016/j.colsurfb.2015.09.017)

14. Mackiewicz M, Rapecki T, Stojek Z, Karbarz M. 2014 Environmentally sensitive, quickly responding microgels with lattice channels filled with polyaniline. *J. Mater. Chem. B* **2**, 1483–1489. (https://doi.org/10.1039/c3tb21578d)

15. Schunicht C, Biffis A, Wulff G. 2000 Microgel-supported oxazaborolidines: novel catalysts for enantioselective reductions. *Tetrahedron* **56**, 1693–1699. (doi:10.1016/S0040-4020(00)00072-7)

16. Hoare T, Pelton R. 2007 Engineering glucose swelling responses in poly(N-isopropylacrylamide)-based microgels. *Macromolecules* **40**, 670–678. (doi:10.1021/ma062254w)

17. Mackiewicz M, Karbarz M, Romanski J, Stojek Z. 2016 An environmentally sensitive three-component hybrid microgel. *Rsc Adv.* **6**, 83 493–83 500. (doi:10.1039/c6ra15048a)

18. Fu Y, Huang Y, Hu JS. 2018 Preparation of chitosan/MCM-41-PAA nanocomposites and the adsorption behaviour of Hg(II) ions. *R. Soc. open sci.* **5**, 171921. (doi:10.1098/rsos.171927)

19. Wisniewska M, Urban T, Grzadka E, Zarko VI, Gun'ko VM. 2014 Comparison of adsorption affinity of polyacrylic acid for surfaces of mixed silica-alumina. *Colloid. Polym. Sci.* **292**, 699–705. (doi:10.1007/s00396-013-3103-x)

20. Bonifacio MA, Cometa S, Dicarlo M, Baruzzi F, de Candia S, Gloria A, Giangregorio MM, Mattioli-Belmonte M, De Giglio E. 2017 Gallium-modified chitosan/poly(acrylic acid) bilayer coatings for improved titanium implant performances. *Carbohydr. Polym.* **166**, 348–357. (doi:10.1016/j.carbpol.2017.03.009)

21. Lin YJ, Hsu FC, Chou CW, Wu TH, Lin HR. 2014 Poly(acrylic acid)-chitosan-silica hydrogels carrying platelet gels for bone defect repair. *J. Biomed. Mater. Res. B Appl. Biomater.* **2**, 8329–8337. (doi:10.1039/c4tb01356e)

22. Goins A, Ramaswamy V, Dirr E, Dulany K, Irby S, Webb A, Allen J. 2018 Development of poly (1,8 octanediol-co-citrate) and poly (acrylic acid) nanofibrous scaffolds for wound healing applications. *Biomed. Mater.* **13**, Artn 015002. (doi:10.1088/1748-605x/aa8439)

23. Calixto G, Yoshii AC, Silva HRE, Cury BSF, Chorilli M. 2015 Polyacrylic acid polymers hydrogels intended to topical drug delivery: preparation and characterization. *Pharm. Dev. Technol.* **20**, 490–496. (doi:10.3109/10837450.2014.882941)

24. Lehr CM. 1994 Bioadhesion technologies for the delivery of peptide and protein drugs to the gastrointestinal-tract. *Crit. Rev. Ther. Drug Carrier Syst.* **11**, 119–160.

25. Shafiei M, Balhoff M, Hayman NW. 2018 Chemical and microstructural controls on viscoplasticity in carbopol hydrogel. *Polymer* **139**, 44–51. (doi:10.1016/j.polymer.2018.01.080)

26. Singh M, Kanoujia J, Parashar P, Arya M, Tripathi CB, Sinha VR, Saraf SK, Saraf SA. 2018 Assessment of improved buccal permeation and bioavailability of felodipine microemulsion-based cross-linked polycarbophil gel. *Drug Deliv. Transl. Res.* **8**, 591–601. (doi:10.1007/s13346-018-0489-5)

27. Dharela R, Kumari S, Chauhan GS, Manuel J, Ahn JH. 2017 Stabilization of uricase by immobilization on poly(acrylic acid)-based nanogels for therapeutic and sensing applications. *Sci. Adv. Mater.* **9**, 1280–1284. (doi:10.1166/sam.2017.2893)

28. Qin YP, Wang HY, He XW, Li WY, Zhang YK. 2018 Metal chelation dual-template epitope imprinting polymer via distillation-precipitation polymerization for recognition of porcine serum albumin. *Talanta* **185**, 620–627. (doi:10.1016/j.talanta.2018.03.082)

29. Pavel FM. 2004 Microemulsion polymerization. *J. Disp. Sci. Technol.* **25**, 1–16. (doi:10.1081/Dis-120027662)

30. Ahmed IN, Chang R, Tsai WB. 2017 Poly(acrylic acid) nanogel as a substrate for cellulase immobilization for hydrolysis of cellulose. *Colloid Surf. B* **152**, 339–343. (doi:10.1016/j.colsurfb.2017.01.040)

31. Modarresi-Saryazdi SM, Haddadi-Asl V, Salami-Kalajahi M. 2018 N,N′-methylenebis(acrylamide)-crosslinked poly(acrylic acid) particles as doxorubicin carriers: A comparison between release behavior of physically loaded drug and conjugated drug via acid-labile hydrazone linkage. *J. Biomed. Mater. Res. A* **106**, 342–348. (doi:10.1002/jbm.a.36240)

32. Yamamoto T, Higashitani K. 2018 Size control of polymeric particle in soap-free emulsion polymerization. *Kona Powder Particle J.* **35**, 66–79. (doi:10.14356/kona.2018012)

33. Wang T, Jin L, Song YN, Li JX, Gao Y, Shi S. 2017 Rheological study on the thermoinduced gelation behavior of poly(N-isopropylacrylamide-co-acrylic acid) microgel suspensions. *J. Appl. Polym. Sci.* **134**, Artn 45259. (doi:10.1002/app.45259)

34. Zhang YP, Liu TH, Wang Q, Zhao JH, Fang J, Shen WG. 2012 Synthesis of novel poly(N,N-diethylacrylamide-co-acrylic acid) (P(DEA-co-AA)) microgels as carrier of horseradish peroxidase immobilization for pollution treatment. *Macromol. Res.* **20**, 484–489. (doi:10.1007/s13233-012-0044-z)

35. Li XT, Zhao D, Shi XD, Qiu G, Lu XH. 2016 Self-assembly and the hemolysis effect of monodisperse N, N-diethylacrylamide/acrylic acid nanogels with high contents of acrylic acid. *Soft Matter* **12**, 7273–7280. (https://doi.org/10.1039/C6SM01537A)

36. Liwinska W, Stanislawska I, Lyp M, Mackiewicz M, Stojek Z, Zabost E. 2017 A degradable nanogel drug carrier crosslinked with three-oligonucleotide hybrids for two-way drug release in mild and high hyperthermia treatment. *J. Mater. Chem. B* **5**, 4713–4724. (doi:10.1039/c7tb00092h)

37. Hoare T, Young S, Lawlor MW, Kohane DS. 2012 Thermoresponsive nanogels for prolonged duration local anesthesia. *Acta Biomater.* **8**, 3596–3605. (doi:10.1016/j.actbio.2012.06.013)

38. Mauser T, Dejugnat C, Sukhorukov GB. 2006 Balance of hydrophobic and electrostatic forces in the pH response of weak polyelectrolyte capsules. *J. Phys. Chem. B* **110**, 20 246–20 253. (doi:10.1021/jp063502t)

39. Zhang QS, Zha LS, Ma JH, Liang BR. 2009 A novel route to prepare pH- and temperature-sensitive nanogels via a semibatch process. *J. Colloid Interface Sci.* **330**, 330–336. (doi:10.1016/j.jcis.2008.09.077)

40. Villamizar-Sarmiento MG, Molina-Soto EF, Guerrero J, Shibue T, Nishide H, Moreno-Villoslada I, Oyarzun-Ampuero FA. 2019 A new methodology to create polymeric nanocarriers containing hydrophilic low molecular-weight drugs: a green strategy providing a very high drug loading. *Mol. Pharmaceut.* **16**, 2892–2901. (doi:10.1021/acs.molpharmaceut.9b00097)

41. Liang Y, Guo YJ, Yang XS, Feng RS, Zhang XM, Li HB. 2019 Insights on the interaction between sodium dodecyl sulfate and partially hydrolyzed microblock hydrophobically associating

polyacrylamides in different polymer concentration regimes. *Colloid Surf. A* **572**, 152–166. (doi:10.1016/j.colsurfa.2019.03.068)

42. Gallardo V, Morales ME, Ruiz MA, Delgado AV. 2005 An experimental investigation of the stability of ethylcellulose latex – correlation between zeta potential and sedimentation. *Eur. J. Pharm. Sci.* **26**, 170–175. (doi:10.1016/j.ejps.2005.05.008)

43. Breite D, Went M, Prager A, Schulze A. 2016 The critical zeta potential of polymer membranes: how electrolytes impact membrane fouling. *Rsc Adv.* **6**, 98 180–98 189. (doi:10.1039/c6ra19239d)

44. Adusumilli M, Bruening ML. 2009 Variation of ion-exchange capacity, zeta potential, and ion-transport selectivities with the number of layers in a multilayer polyelectrolyte film.

Langmuir **25**, 7478–7485. (doi:10.1021/la900391q)

45. Szewczuk-Karpisz K, Krasucka P, Boguta P, Skic K, Sokolowska Z, Fijalkowska G, Wisniewska M. 2019 Anionic polyacrylamide efficiency in goethite removal from aqueous solutions: goethite suspension destabilization by PAM. *Int. J. Environ. Sci. Technol.* **16**, 3145–3154. (doi:10.1007/s13762-018-2064-5)

46. Cho D, Lee S, Frey MW. 2012 Characterizing zeta potential of functional nanofibers in a microfluidic device. *J. Colloid Interface Sci.* **372**, 252–260. (doi:10.1016/j.jcis.2012.01.007)

47. Temmel S, Kern W, Luxbacher T. 2006 Zeta potential of photochemically modified polymer surfaces. *Prog. Coll. Pol. Sci.* **132**, 54–61. (doi:10.1007/2882_032)

48. Wolff HJM, Kather M, Breisig H, Richtering W, Pich A, Wessling M. 2018 From batch to continuous precipitation polymerization of thermoresponsive microgels. *ACS Appl. Mater. Interfaces* **10**, 24 799–24 806. (doi:10.1021/acsami.8b06920)

49. Wu HQ *et al.* 2017 Synergistic cisplatin/doxorubicin combination chemotherapy for multidrug-resistant cancer via polymeric nanogels targeting delivery. *ACS Appl. Mater. Interfaces* **9**, 9426–9436. (doi:10.1021/acsami.6b16844)

50. Es-haghi H, Bouhendi H, Bagheri-Marandi G, Zohurian-Mehr MJ, Kabiry K. 2010 Cross-linked poly(acrylic acid) microgels from precipitation polymerization. *Polym. Plast. Technol. Eng.* **49**, 1257–1264. (doi:10.1080/03602559.2010.496421)